Chapter 10
A Circumpolar Perspective on the Contribution of Trees to the Boreal Forest Carbon Balance

Christoforos Pappas, Flurin Babst, Simone Fatichi, Stefan Klesse, Athanasios Paschalis, and Richard L. Peters

Abstract Partitioned estimates of the boreal forest carbon (C) sink components are crucial for understanding processes and developing science-driven adaptation and mitigation strategies under climate change. Here, we provide a concise tree-centered overview of the boreal forest C balance and offer a circumpolar perspective on the contribution of trees to boreal forest C dynamics. We combine an *ant's-eye* view, based on quantitative in situ observations of C balance, with a *bird's-eye* perspective on C dynamics across the circumboreal region using large-scale data sets. We conclude with an outlook addressing the trajectories of the circumboreal C dynamics in response to projected environmental changes.

C. Pappas (✉)
Department of Civil Engineering, University of Patras, 26504 Rio Patras, Greece
e-mail: cpappas@upatras.gr

Centre for Forest Research, Université du Québec à Montréal, P.O. Box 8888, Stn. Centre-Ville, Montréal, QC 3C 3P8, Canada

Département Science et Technologie, Université TÉLUQ, 5800 rue Saint-Denis, Montréal, QC 2S 3L5, Canada

F. Babst
School of Natural Resources and the Environment, Laboratory of Tree-Ring Research, The University of Arizona, 1046 E Lowell St, Tucson, AZ 85721, USA
e-mail: babst@arizona.edu

S. Fatichi
Department of Civil and Environmental Engineering, College of Design and Engineering, National University of Singapore, 1 Engineering Drive 2, Block E1A #05-12, Singapore 117576, Singapore
e-mail: ceesimo@nus.edu.sg

S. Klesse
Forest Dynamics, Swiss Federal Research Institute for Forest, Snow and Landscape Research WSL, Zürcherstrasse 111, 8903 Birmensdorf, Switzerland
e-mail: stefan.klesse@wsl.ch

A. Paschalis
Department of Civil and Environmental Engineering, Imperial College London, South Kensington Campus London, Skempton Building, SW7 2AZ London, UK
e-mail: a.paschalis@imperial.ac.uk

10.1 Introduction

One of the many services that forest ecosystems offer to humanity is the absorption of atmospheric CO_2 and its conversion to chemical energy stored as biomass. Plant biomass, which has about 50% carbon (C) content, represents the largest biomass pool of the biosphere (Bar-On et al., 2018). In the Anthropocene, characterized by continuously increasing anthropogenic CO_2 emissions, this forest C sink has been a particularly important yet vulnerable component of the terrestrial C balance and a fundamental ecosystem service. Forests have a pronounced effect on the Earth's biogeochemical cycles and climate system (e.g., Bonan, 2008; Ciais et al., 2019; Friedlingstein, 2015). The latest estimates report that the land C sink amounts to about three Pg C·yr^{-1} (where 1 Pg equals 10^{15} g), which corresponds to an average of 25 g C·yr^{-1} stored per square meter of vegetated land (Fatichi et al., 2019; Le Quéré et al., 2018). Attributing the terrestrial C sink to specific components and their inherent processes is important and topical, not only for a better understanding and modeling of the biogeochemical cycles under climate change but also for applying science-driven adaptation and mitigation strategies (Duncanson et al., 2019; Friedlingstein et al., 2020; Grassi et al., 2018; Kurz et al., 2013).

Natural management solutions, like tree planting and forest regrowth or densi-fication, have been advocated as viable approaches for removing a fraction of the continuously increasing anthropogenic CO_2 emissions (Cook-Patton et al., 2020). However, concerns have been raised regarding the efficacy of such natural solutions, as biophysical (e.g., energy, water, and nutrient availability) and ecological (e.g., self-thinning) theory provides well-known constraints on a tree's capacity to grow, thrive, and sequester C (Baldocchi & Peñuelas, 2019; Popkin, 2019). Moreover, the long-term strength of this C sink is also shaped by disturbance dynamics and the turnover rates of the different C pools, e.g., leaves and roots, which span a large range of temporal scales, i.e., C residence times, rather than tree growth per se (Bugmann & Bigler, 2011; Carvalhais et al., 2014; Clemmensen et al., 2013; Friend et al., 2014; Harmon, 2001; Körner, 2017; Yu et al., 2019). Thus, disentangling the C balance pools could facilitate a robust and quantitative description of the C sink strength and its fate under global change (Anderegg et al., 2020; Brienen et al., 2020; Büntgen et al., 2019; Duchesne et al., 2019; Pugh et al., 2019b).

The circumboreal region represents a massive amount of land (ca. 33% of the Earth's forested area); thus, understanding and quantifying its C balance is extremely

R. L. Peters

Laboratory of Plant Ecology, Department of Plants and Crops, Faculty of Bioscience Engineering, Ghent University, Coupure links 653, 9000 Ghent, Belgium
e-mail: richard.peters@unibas.ch

Forest Is Life, TERRA Teaching and Research, Gembloux Agro Bio-Tech, University of Liège, Avenue de la Faculté d'Agronomie, B-5030 Gembloux, Belgium

Physiological Plant Ecology, Department of Environmental Sciences, University of Basel, Schönbeinstrasse 6, CH-4056 Basel, Switzerland

critical for both science and policymaking. Boreal forests constitute the largest C storage pool in the extratropics, with a total biomass stock of 270 Pg C, the largest fraction of which is stored belowground—218 Pg C, as soil organic matter, litter, fine and coarse roots (Pan et al., 2013). About 0.74 trillion trees grow in the boreal region (Crowther et al., 2015), with a total living aboveground biomass (overstory vegetation) of approximately 54 Pg C, having an average biomass density of 5 kg C·m^{-2} (Pan et al., 2013). Ongoing environmental changes, including a higher frequency and intensity of transient disturbances (e.g., droughts, heat waves, fires, and insect outbreaks) and persistent changes (e.g., permafrost thaw and the warming and associated shifts in spring and autumn phenology) affect boreal forest C sink strength (Amiro et al., 2010; Bradshaw & Warkentin, 2015; Pugh et al., 2019a; Seidl et al., 2017). Such changes in the C cycle also impact the intrinsically coupled water and energy cycles and could trigger numerous feedbacks to the climate system at local, regional, and global scales.

Numerical models, supported by novel monitoring techniques, allow us to quantify the forest C balance and its components. However, observations and mechanistic models, e.g., the biochemical model of photosynthesis (Farquhar et al., 1980), are much more refined for aboveground processes than belowground ones. This reflects a bias imposed by the ease of measuring certain variables, e.g., aboveground vegetation monitoring with direct measurements, forest surveys, and remote sensing, compared with the variables and dynamics of belowground biogeochemical processes, which are more challenging to observe (e.g., Körner, 2018). From a C balance perspective, whereas tree stature, leaf area, and the biochemical properties of foliage define the C supply (source), it is the interplay with the belowground resources, e.g., water and nutrient availability, and the environment, e.g., temperature, that shape tree growth (sink) and ecosystem C partitioning at intra- and interannual time scales (e.g., Fatichi et al., 2019).

Here, we provide a concise overview of the magnitude and variability of boreal forest C fluxes and offer a circumpolar perspective on the contribution of trees to the boreal forest C balance. We deliberately provide a tree-centered perspective and focus mainly on vegetation physiological processes (e.g., Babst et al., 2021). Yet, forest management, natural disturbances (e.g., fires, insect outbreaks, and permafrost thaw), and forest demography, all of which are not discussed here, are fundamental coregulators of boreal forest structure and functioning and have pronounced implications for the boreal forest C sources and sinks (Anderegg et al., 2020; Brassard & Chen, 2006; McDowell et al., 2020). We combine an *ant's-eye* view, based on quantitative in situ observations of the component C fluxes and pools within three boreal forests—spanning from eastern Siberia to Finland to central Canada—with a *bird's-eye* perspective on C dynamics across the circumboreal region using spatially explicit state-of-the-art remote-sensing and machine-learning data sets. The compiled literature illustrates the importance of tree physiological processes in shaping the tree-level C balance and the interplay with belowground processes in regulating the C balance at the landscape and ecosystem levels. We conclude with an outlook on the potential trajectories

of C dynamics in the circumboreal region in response to the projected increase in air temperature, vapor pressure deficit, and atmospheric CO_2 concentration, on the basis of a tree-level physiological understanding and large-scale observational evidence.

10.2 Forest Carbon Balance and Its Components

The terrestrial C sink is often quantified by net ecosystem production (NEP), which is the difference between two large fluxes: the C assimilated through photosynthesis (C input), which at the ecosystem level is referred to as gross ecosystem production (GEP), and the C that is released to the atmosphere as ecosystem respiration (R_{eco}; C output), i.e., the sum of autotrophic (R_a) and heterotrophic (R_h) respiration components (Fig. 10.1; Chapin et al., 2006; Fatichi et al., 2019; Keenan & Williams, 2018; Manzoni et al., 2018). If the balance of these two fluxes is positive, i.e., NEP = GEP – R_{eco} > 0, then the ecosystem is a C sink. The net primary production (NPP = GEP – R_a) corresponds to the assimilated C that is invested into structural biomass growth, root exudates, nonstructural carbohydrates, and biogenic volatile organic compounds. When NPP is expressed as a fraction of GEP, it provides an integrated metric of ecosystem carbon use efficiency (CUE), i.e., CUE = NPP/GEP = 1 – (R_a/GEP) (Fatichi et al., 2019; Manzoni et al., 2018). Several methods exist for measuring and inferring the components of the C balance (Fig. 10.1). They include (1) the eddy covariance technique (Baldocchi, 2020) used to measure the forest-stand level net exchange of CO_2 between the land surface and the atmosphere, i.e., net ecosystem exchange (NEE), where NEE = –NEP in the absence of lateral C fluxes and major disturbances, and to infer the component C fluxes, i.e., GEP and R_{eco} (Reichstein et al., 2005); (2) repeated inventories of permanent forest monitoring plots to derive area-based C fluxes and pools (Anderson-Teixeira et al., 2015; Clark et al., 2001); (3) gas exchange chambers, e.g., enclosing specific soil patches or tree organs or entire plants or trees (Drake et al., 2019); and (4) biometric methods for reconstructing aboveground tree growth at the forest-stand level from tree-ring widths, allometric relationships, and information on forest-stand demography (e.g., Campioli et al., 2016). In addition, recent technological advancements in airborne and satellite remote sensing, e.g., NASA's GEDI mission; https://gedi.umd.edu/, and multivariate data synthesis initiatives, e.g., the Forest Observation System initiative, http://forest-observation-system.net/, offer spatially explicit products of C fluxes and pools worldwide (Rodríguez-Veiga et al., 2019; Schepaschenko et al., 2019; Thurner et al., 2014).
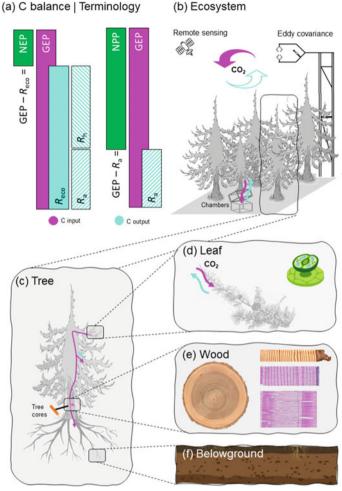
Fig. 10.1 a An overview of the terrestrial carbon (C) balance and common measuring techniques at the **b** ecosystem, **c** tree, and organ level, including **d** leaf, **e** wood, and **f** roots. **a** Ecosystem-level C input (gross ecosystem production; GEP) and output (ecosystem respiration, R_{eco}, and its components, namely autotrophic, R_a, and heterotrophic, R_h, respiration) and the resulting C fluxes (net primary production (NEP) and net primary productivity (NPP)); **b** ecosystem-level C fluxes and pools can be estimated through remote sensing and the eddy covariance technique, and, when combined with tree-level measurements and chamber techniques, a partition of C fluxes and pools can be derived; **c** tree rings, when combined with auxiliary biometric measurements, can reconstruct aboveground tree biomass increments, thereby assessing how **d** leaf-level C assimilation is translated into **e** stem biomass or **f** translocated to belowground tree C pools

10.3   Ant's-Eye View

To illustrate the dynamics of the boreal forest C balance, we selected three sites having well-documented estimates of C fluxes and pools that cover an extensive longitudinal gradient from eastern Siberia to Finland to central Canada (Table 10.1 and Fig. 10.2). We compiled estimates of R_{eco} and its component fluxes (i.e., R_a and R_h), GEP, NEP, NPP, and the aboveground tree biomass increments (AGBi) at these sites (Fig. 10.1). These values were derived with the eddy covariance technique, biometric/inventory-based approaches, gas exchange chamber methods, or a combination thereof. The selected sites provide not only a circumboreal perspective across three continents but also include distinct boreal tree species compositions, namely larch-, pine-, and spruce-dominated landscapes, which occupy vast areas of the boreal region (Table 10.1 and Fig. 10.2).

10.3.1   Site Description

At the eastern limit of the longitudinal gradient, the example site is a larch (*Larix cajanderi* Mayr) dominated forest stand in Siberia (fluxnet ID: RU-SKP; Yakutsk Spasskaya Pad larch; Table 10.1). This site is part of the Spasskaya Pad Scientific Forest Station of the Institute for Biological Problems of the Cryolithozone and is situated 20 km north of Yakutsk in the Republic of Sakha, Russia (62.26°N, 129.17°E; 246 m asl). The overstory consists mainly of larch, with sporadic occurrences of willow (*Salix* spp.) and silver birch (*Betula pendula* Roth), whereas the forest floor is covered with dense cowberry (*Vaccinium vitis-idaea* L.). Stand density is 840 stem·ha^{-1} (Tei et al., 2019). The leaf area index (LAI), canopy height, and stand age are equal to 1.5 m^2·m^{-2}, 20 m, and 190 yr, respectively (Kotani et al., 2014). The site lies in the continuous permafrost zone and has sandy loam soils. Mean annual air temperature and total precipitation at the site are –9 °C and 237 mm, respectively (Tei et al., 2019). We used published values of the growing season (May–September) GEP from Tei et al. (2019), collected between 2004 and 2014 with the eddy covariance technique. A detailed description of the micrometeorological and eddy covariance instrumentation at the site and the eddy covariance processing methods used for deriving GEP are provided in Ohta et al. (2008, 2014), Kotani et al. (2014), and Tei et al. (2019). Ecosystem respiration at the site was estimated as 75% of GEP, and NEP amounts to 25% of GEP (Kotani et al., 2014). Furthermore, R_h was estimated as 52% of GEP (Sawamoto et al., 2003), and R_a was then calculated as $R_{eco} - R_h$. This allowed us to derive partitioned C fluxes at the site for the 2004–2014 period. We complemented these variables with tree-ring-derived AGBi estimates for the 1990–2013 period (S. Klesse; unpublished results, https://www.ncei.noaa.gov/acc ess/paleo-search/study/34312). Specifically, AGBi time series were derived with a biometric approach (Babst et al., 2014a, b) by combining ring widths from tree cores sampled in 2014, species-specific allometry, and stand density information
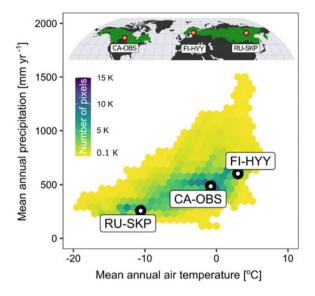
Table 10.1 An overview of the three examined boreal forest stands, including their location, climatic conditions (mean annual temperature, MAT, and total precipitation, MAP), vegetation characteristics (leaf area index, LAI), and carbon fluxes and pools, namely autotrophic (R_a) and heterotrophic respiration (R_h), ecosystem respiration (R_{eco}), gross ecosystem production (GEP), net primary production (NPP), net ecosystem production (NEP), and aboveground biomass increment (AGBi). The evaluated period is in parentheses

Location			
Site name	Yakutsk Spasskaya Pad Larch	Hyytiälä	Southern Old Black Spruce
Site ID	RU-SKP	FI-HYY	CA-OBS
Longitude (°)	129.17	24.30	−105.12
Latitude (°)	62.26	61.85	53.98
Elevation (m a.s.l.)	256	181	629
DOI	https://doi.org/10.18140/FLX/1440243	https://doi.org/10.18140/FLX/1440158	https://doi.org/10.18140/FLX/1440044
Climatic conditions			
MAT (°C)	−9[a]	4.4[h]	1.4
MAP (mm)	237[a]	604[h]	428
Vegetation characteristics			
Overstory vegetation	*Larix cajanderi*	*Pinus sylvestris*	*Picea mariana*
Density (stems·ha^{-1})	840[a]	1,373 (2008)[e]	5,921 (2016)[j]
Basal area (m^2·ha^{-1})	24[b]	23 (2008)[e]	38 (2016)[j]
Stand age (yr)	190[b]	47 (2009)[f]	140[k]
Canopy height (m)	20[b]	15 (2008)[e]	16 (2005)[l]
LAI (m^2·m^{-2})	1.5[b]	2.5 (1995)[g]	3.8 (2005)[l]
Carbon fluxes and pools			
GEP (g C·m^{-2}·yr^{-1})	635 ± 73 (2004–2014)[a]	1,169 ± 152 (1996–2014)[h]	809 ± 50 (1999–2015)[j,m]

(continued)

Table 10.1 (continued)

Location			
NEP (g C·m^{-2}·yr^{-1})	159 ± 18 (2004–2014)[a,b]	246 ± 148 (1996–2014)[h]	40 ± 23 (1999–2015)[j,m]
NPP (g C·m^{-2}·yr^{-1})	489 ± 56 (2004–014) based on GEP and R_a	643 ± 84 (1996–2014)[i]	405 ± 27 (1999–2015)[j,m]
R_{eco} (g C·m^{-2}·yr^{-1})	477 ± 55 (2004–2014)[a,b]	927 ± 83 (1996–2014)[h]	769 ± 56 (1999–2015)[j,m]
R_h (g C·m^{-2}·yr^{-1})	330 ± 38 (2004 –2014)[c]	401 ± 54 (1996–2014)[i]	365 ± 14 (1999–2015)[j,m]
R_a (g C·m^{-2}·yr^{-1})	146 ± 17 (2004–2014)[f]; using R_{eco} and R_h from above	526 ± 69 (1996–2014)[i]	404 ± 45 (1999–2015)[j,m]
AGBi (g C·m^{-2}·yr^{-1})	26 ± 9 (1990–2013)[d]	97 ± 12 (1996–2009)[f]	71 ± 7 (1999 − 2015)[j,m]
AGBi/GEP (%)	4.1	8.3	8.8

[a]Tei et al. (2019), [b]Kotani et al. (2014), [c]Sawamoto et al. (2003), [d]this study, [e]Ilvesniemi et al. (2009), [f]Babst et al. (2014a), [g]Mencuccini and Bonosi (2001), [h]FLUXNET2015, [i]Pumpanen et al. (2015), [j]Pappas et al. (2020), [k]Krishnan et al. (2008), [l]Chen et al. (2006), [m]Liu et al. (2019)

Fig. 10.2 Climate envelope of the boreal forest ecozone and the location of the three example boreal forest sites in the two-dimensional climate space of mean annual air temperature and total precipitation; *hexagons*, color-coded with the density of 5′ resolution pixels, define the climate space of mean annual air temperature and total precipitation, as quantified using the WorldClim version 2.1 data set (long-term mean for 1970–2000; Fick & Hijmans, 2017). The circumpolar boreal forest extent (*dark green* in the upper panel) follows the definition of the World Wildlife Fund terrestrial ecoregions map and was downloaded from http://glad.geog.umd.edu/projects/gfm/boreal/data.html. *Note* that a lower cutoff of 100 pixels was applied to enhance the figure's clarity

(Sawamoto et al., 2003). Mass values were converted into C units using a 47% C concentration proposed in the literature for larch stemwood (Alexander et al., 2012).

In Europe, we selected a Scots pine (*Pinus sylvestris* L.)–dominated forest in southern Finland, located 200 km north of Helsinki (Hyytiälä; 61.85°N, 24.30°E; 181 m asl; Table 10.1). This is a long-term experimental forest site operated by the University of Helsinki (Station for Measuring Forest Ecosystem-Atmosphere Relations, SMEAR II; fluxnet ID: FI-HYY). Long-term (1996–2014) mean annual air temperature and total precipitation at the site are 4.4 °C and 604 mm, respectively. Stand density is 1,373 stems ha^{-1}, and average canopy height, LAI, and stand age are 15 m, 2.5 m^2 m^{-2} and 47 years, respectively (Babst et al., 2014a; Ilvesniemi et al., 2009; Mencuccini & Bonosi, 2001). Overstory vegetation consists of Scots pine (>95%) with the sporadic occurrence of Norway spruce (*Picea abies* (L.) H. Karst) and silver birch. The understory vegetation is considered negligible because of local forest management practices. The ground cover consists mainly of blueberry (*Vaccinium myrtillus* L.), cowberry, small-reed (*Calamagrostis epigejos* (L.) Roth), heather (*Calluna vulgaris* (L.) Hull), and feather mosses (*Pleurozium schreberi* (Brid.) Mitt., *Dicranum polysetum* Sw.). The soils are mineral on glacial till over a homogeneous bedrock; sporadic peat soils are found in the depressions (Kolari et al.,

2009; Pumpanen et al., 2015). Here, we used eddy covariance–derived estimates of NEP, GEP, and R_{eco} for the 1996–2014 period, as provided by the FLUXNET2015 data set (Pastorello et al., 2020). Combining these eddy covariance–derived estimates with the detailed site-level forest C balance presented in Ilvesniemi et al. (2009) and Pumpanen et al. (2015), we derived average values of NPP, R_a, and R_h. More specifically, R_a was estimated as 45% of GEP; R_h was then calculated as $R_{eco} - R_a$, and NPP was computed as GEP $- R_a$ (Pumpanen et al., 2015). Moreover, tree contribution to the forest C balance was quantified using the AGBi time series presented in Babst et al., (2014a, 2014b). This allowed us to derive partitioned C fluxes at the site for the 1996–2014 period. Detailed descriptions of the micrometeorological and eddy covariance instrumentation at the site and data processing documentation can be found in Rannik et al. (2002) and Vesala et al. (2005).
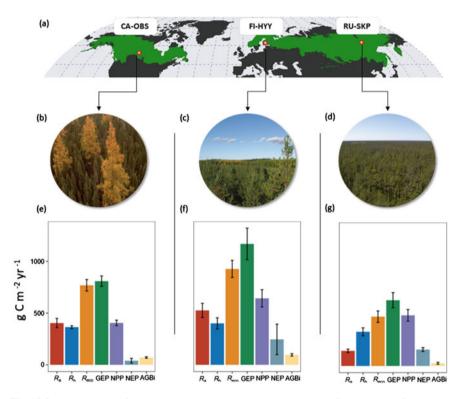
The Canadian site is located near the southern edge of the boreal forest in Saskatchewan, Canada (Southern Old Black Spruce, fluxnet ID: CA-OBS; 53.98°N, 105.12°W; 629 m asl; Table 10.1). Long-term (1981–2010) mean annual air temperature and total precipitation in the area are 1.4 °C and 428 mm, respectively (Pappas et al., 2020). Stand age is ca. 140 years—initiated after a fire in ca. 1879 (Krishnan et al., 2008; Liu et al., 2019). The overstory consists mainly of mature black spruce (*Picea mariana* (Mill.) BSP) mixed with sporadic mature eastern larch (*Larix laricina* (Du Roi) K. Koch). The average LAI at the site is 3.8 m^2·m^{-2} (Chen et al., 2006). Wild rose (*Rosa woodsii* Lindl.) and Labrador tea (*Rhododendron groenlandicum* (Oeder) Kron & Judd) are the dominant woody shrubs, and the ground cover consists mainly of mixed feather mosses (*Hylocomium splendens* (Hedw.) Schimp., *Pleurozium schreberi*, and *Ptilium crista-castrensis* (Hedw.) De Not.) with some peat moss (*Sphagnum* spp.) and lichen (*Cladina* spp.) (Gaumont-Guay et al., 2014). The soil is moderately to poorly drained with a 20 to 30 cm thick peat layer overlying waterlogged sand (Barr et al., 2012; Gower et al., 1997; Griffis et al., 2003). The recent study of Liu et al. (2019) provides a detailed overview of the partitioned C fluxes at the site during the last decades (1999–2017), including GEP, NEP, R_{eco}, R_a, and R_h, by combining long-term eddy covariance measurements with automatic chamber measurements. Furthermore, Pappas et al. (2020) present reconstructed estimates of AGBi at the site using a biometric approach, i.e., tree cores collected with a biomass upscaling design and species-specific allometry, similar to the one followed in the AGBi estimates at the other two sites, detailed above. Here, we used published values of the partitioned C fluxes and pools from Pappas et al. (2020), focusing on 1999 to 2015.

10.3.2 Ecosystem Carbon Balance and the Impact of Environmental Conditions

The selected forest sites offer a perspective on the magnitude and variability of boreal forest C fluxes and pools and illustrate the numerous interactions between biotic,

e.g., species composition, and abiotic factors, e.g., local climate and stand demography, that can shape site-level C dynamics (Fig. 10.3). The long-term measurements revealed that the study sites were C sinks during the last decade, i.e., NEP > 0, yet the sink strength at each site varied from 40 ± 23 g C·m^{-2}·yr^{-1} at CA-OBS to 246 ± 148 g C·m^{-2}·yr^{-1} at FI-HYY (hereafter, the presented values correspond to mean $\pm$ one standard deviation; Table 10.1).

The long-term mean annual GEP across the three locations followed a climatological gradient (Figs. 10.2 and 10.3); the highest value of GEP corresponded to the site having the most favorable climatological conditions, i.e., highest mean annual air temperature and precipitation at FI-HYY; GEP = $1,169 \pm 152$ g C·m^{-2}·yr^{-1}, whereas the lowest values of GEP coincided with the Siberian site where mean annual air temperature and precipitation were lowest (RU-SKP; GEP = 635 ± 73 g C·m^{-2}·yr^{-1}; Figs. 10.2 and 10.3). Similarly, AGBi across FI-HYY, CA-OBS, and RU-SKP ranged

Fig. 10.3 An overview of the carbon balance components at the three reference boreal forest sites. **a** Circumboreal forest extent with the three sites indicated in *red*; **b, c,** and **d** the forest canopy as seen from the top of the eddy covariance tower at the sites; **e, f,** and **g** carbon balance components as compiled from the literature, namely autotrophic (R_a) and heterotrophic respiration (R_h), ecosystem respiration (R_{eco}), gross ecosystem production (GEP), net primary production (NPP), net ecosystem production (NEP), and aboveground biomass increment (AGBi)

from 97 ± 12 g C·m^{-2}·yr^{-1} to 71 ± 7 g C·m^{-2}·yr^{-1} to 26 ± 9 g C·m^{-2}·yr^{-1}, respectively, following the decrease in mean annual precipitation and temperature across the sites (Fig. 10.2). However, apart from the prevailing climatological conditions, both ecosystem-level production (GEP) and tree-level stem growth (AGBi) can be affected by numerous other factors explaining the reported differences across the examined forest stands. Such factors include site-specific biophysical constraints, e.g., stand density and LAI, as well as differences in demography and species composition, tree ontogeny (e.g., stand age ranging from 190 yr at RU-SKP to 47 yr at FI-HYY), and phenology (e.g., deciduous larch at RU-SKP versus evergreen spruce and pine at CA-OBS and FI-HYY, respectively), and soil biochemistry (Table 10.1). The impact of these biotic and abiotic factors manifests in the cross-site variability of the long-term component C fluxes. Importantly, while R_{eco}, R_a, and R_h decreased across the three sites with a pattern comparable to that of GEP, NEP and NPP did not follow this pattern. At RU-SKP, NEP and NPP were higher than at CA-OBS (Table 10.1) because of the balance between GEP, R_{eco}, and R_a. It is worth noting that the components of C fluxes were derived as a constant fraction of GEP at RU-SKP because of data scarcity. Thus, the estimates of NEP, NPP, R_{eco}, R_a, and R_h are more uncertain than estimates at both FI-HYY—where NEP and GEP values were available and only NPP, R_a, and R_h were derived as constant fractions—and CA-OBS, where all component C fluxes and pools were obtained directly from measurements.

10.3.3 Limited Contribution of Aboveground Tree Growth to the Ecosystem Carbon Sink

The C allocated to aboveground tree growth accounted for less than 10% of the total ecosystem C input at the study sites (Table 10.1), with the lowest fraction of GEP allocated to aboveground stem growth reported at the RU-SKP site (AGBi/GEP = 4.1%) and the highest fraction at CA-OBS (AGBi/GEP = 8.8%). In central and northeastern Siberia, Kajimoto et al. (2010) provided insights from larch-dominated stands and reported values of total biomass increments (i.e., stem, branches, and needles) and aboveground NPP for young stands (<30 yr) equal to 54 g C·m^{-2}·yr^{-1} and 95 g C·m^{-2}·yr^{-1} and for old stands (>100 yr) equal to 15 g C·m^{-2}·yr^{-1} and 34 g C·m^{-2}·yr^{-1}, respectively. The estimates of AGBi reported here for the old intact forest stand at RU-SKP (190 yr; Table 10.1) agree well with these findings and highlight the low aboveground growth rates of Siberian larch forest stands compared with the southern boreal sites in Europe and North America. At a pine-dominated site in Siberia, Lloyd et al. (2002) reported AGBi/GEP $\approx$ 16%, which is comparatively larger than our estimate at RU-SKP but within the expected range of AGBi/GEP variability in the boreal region (Pappas et al., 2020). Permafrost conditions and waterlogging in eastern Siberia have been identified as key factors affecting ecosystem-level C fluxes and forest structure and health (Kotani et al., 2014; Ohta et al., 2014). The estimates of AGBi and the resulting fractions of AGBi/GEP are also well constrained

at CA-OBS and agree well with previously published studies and auxiliary observations, e.g., forest inventories and remote-sensing products, from the same site, e.g., AGBi $\approx$ 110 g C·m^{-2}·yr^{-1}, therefore 11% of GEP (Malhi et al., 1999), and other boreal forest sites in North America (see Pappas et al. (2020) and references therein). Some discrepancy exists, however, in the AGBi estimates at FI-HYY. Ilvesniemi et al. (2009) reported a larger contribution of C accumulation into the aboveground tree biomass at FI-HYY, i.e., AGBi $\approx$ 240 g C·m^{-2}·yr^{-1} for the period 1995 to 2008, when compared with the estimates from Babst et al., (2014a, 2014b) used here. This discrepancy could be associated with methodological differences between the two studies, especially in regard to stand density and species-specific biomass allometry. Furthermore, Lagergren et al. (2019) combined eddy covariance observations with annual biomass increments in a mixed pine-spruce forest in the southern part of the boreal region of Sweden and found that out of the 957 g C·m^{-2}·yr^{-1} of mean annual GEP, stem growth accounted for ~14%, i.e., AGBi $\approx$ 137 g C·m^{-2}·yr^{-1}. The low fraction of GEP allocated to aboveground tree growth in the boreal region underlines the relatively high rates of R_a, the important belowground tree C investments, and also the role of understory vegetation for the boreal forest C balance (Bradshaw & Warkentin, 2015; Clemmensen et al., 2013; Hart & Chen, 2006). Additionally, boreal forest soils are often nutrient poor, potentially explaining the priority for trees to invest in belowground components, including fine roots, root exudates, and mycorrhizae (Chapin, 1980; Clemmensen et al., 2013; Vicca et al., 2012).
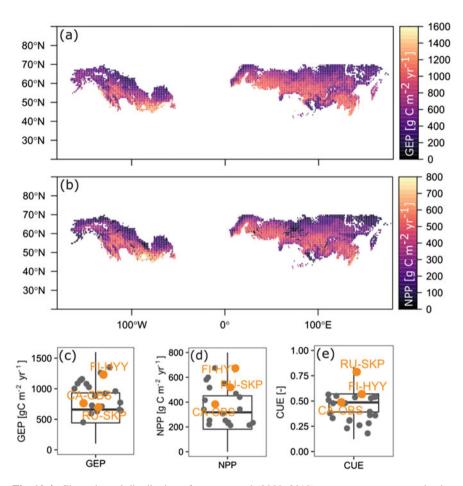
10.4   Bird's-Eye View

We complemented the in situ measurements of the component C fluxes and pools with long-term estimates of GEP and NPP from two recently developed global data sets. We used mean (2000–2019) annual (a) GEP derived by upscaling eddy covariance data from the FLUXNET2015 data set (Pastorello et al., 2020) with random-forest machine-learning algorithms (Zeng et al., 2020) and (b) NPP from MODIS remote-sensing algorithms (https://lpdaac.usgs.gov/products/mod17a3hgfv006/; Running & Zhao, 2019). Both products were resampled to a 0.1° spatial resolution and extracted over the circumboreal region (http://glad.geog.umd.edu/projects/gfm/boreal/data.html). Although such global products lack the direct constraint and accuracy of in situ observations, as presented in the previous section, they can illustrate relevant spatial patterns and provide a "bird's eye" circumboreal perspective on forest C dynamics.

Across the circumboreal region, GEP and NPP are 692 $\pm$ 299 g C·m^{-2}·yr^{-1} and 319 $\pm$ 163 g C·m^{-2}·yr^{-1}, respectively. The circumboreal distribution of GEP and NPP frames an envelope for the in situ partitioned C fluxes presented here and in the recent meta-analysis of Pappas et al. (2020). More specifically, across the 21 boreal forest sites synthesized in Pappas et al. (2020), GEP and NPP were 898 $\pm$ 251 g C·m^{-2}·yr^{-1} and 373 $\pm$ 153 g C·m^{-2}·yr^{-1}, respectively, with the estimates at the three sites examined here falling within this range (Fig. 10.4). Yet, it is worth

mentioning that the site-specific GEP and NPP observations correspond mainly to southern boreal forest sites; this explains their higher values compared with those estimated across the entire circumboreal region (Fig. 10.4).

The inferred remotely sensed CUE across the circumboreal region varied around 0.47 ± 0.15 (Fig. 10.4), with the site-level estimates compiled in Pappas et al. (2020) pointing toward a lower mean value (i.e., 0.40 ± 0.12). At the three sites examined here, CUE was equal to 0.77, 0.55, and 0.50 for RU-SKP, FI-HYY, and CA-OBS,

Fig. 10.4 Circumboreal distribution of mean annual (2000–2019) **a** gross ecosystem production (GEP), estimated using machine-learning and eddy covariance data (Zeng et al., 2020) and **b** net primary production (NPP) obtained from remote sensing (MODIS/TerraMOD17A3HGFv006; https://lpdaac.usgs.gov/products/mod17a3hgfv006/; Running & Zhao, 2019). The spatial resolution of the presented maps is $0.1°$. Box plots of **c** GEP, **d** NPP, and **e** carbon use efficiency (CUE), CUE = NPP/GEP, across the circumboreal region using data presented in subplots **a** and **b**. Points within the box plots denote the estimates at the three example locations (*orange*) and a synthesis of boreal forest sites (*gray*) from the meta-analysis of Pappas et al. (2020)

respectively (Fig. 10.4). The high value of CUE at RU-SKP and the circumboreal estimates of CUE from the global products of NPP and GPP falling outside the interquartile range are most likely explained by observational uncertainties. More specifically, partitioned respiration fluxes (R_h and R_a) at RU-SKP were not estimated with independent methods but rather using fixed fractions of GEP, e.g., for R_h. Although such fixed fractions are supported by the available site-specific literature and are also expected because of biophysical constraints—R_h and R_a should be large and constrained fractions of productivity (Baldocchi & Peñuelas, 2019)—the resulting CUE at RU-SKP seems unrealistically high. Moreover, in situ GEP estimates in the circumboreal region are generally scarce, thereby resulting in poorly constrained predictions using machine-learning techniques across these regions, potentially explaining the reported discrepancy.

Theoretical, observational, and modeling insights point toward a well-constrained variability of CUE worldwide, with a mean value around 0.46 (Collalti & Prentice, 2019; De Lucia et al., 2007; Dewar et al., 1998; Fatichi et al., 2019; Landsberg et al., 2020; Litton et al., 2007; Van Oijen et al., 2010; Waring et al., 1998). Boreal forests are expected to manifest lower CUE values relative to those of other biomes because of lower overall productivity and higher rates of C loss during the dormant season (De Lucia et al., 2007). As recently summarized by Landsberg et al. (2020), CUE estimates outside the 0.4 to 0.6 range are unlikely and can be associated with an inaccurate assessment of NPP, especially in regard to belowground components such as fine roots, root exudates, and mycorrhizae (Chapin, 1980; Clemmensen et al., 2013; Vicca et al., 2012). However, the variability of ecosystem-level CUE in the 0.4 to 0.6 range can be explained by site-level differences in soil nutrition, stand demography, and stand ontogeny. More specifically, with increasing stand age and canopy closure, CUE is expected to decrease because of a saturation in GEP and higher rates of R_a (Brassard & Chen, 2006; De Lucia et al., 2007; Odum, 1969). Thus, site-level stand demography, disturbance history, and differences in soil fertility could explain some of the spatial patterns illustrated in Fig. 10.4.

10.5   Synthesis and Outlook

The circumboreal region provides habitat for flora and fauna and crucial ecological, social, economic, and spiritual services (e.g., Gauthier et al., 2015; Trumbore et al., 2015). In addition to these benefits, boreal forests provide a substantial C sink and regulate numerous land–atmosphere interactions and feedbacks to the climate system, e.g., sensible/latent heat, albedo feedback, and runoff/evapotranspiration partitioning; Bonan, 2008; Reichstein et al., 2013. Thus, a predictive understanding of boreal forests' growth trajectories could provide quantitative insights for comprehensive climate policy recommendations (Bonan, 2016; Kurz et al., 2013). The scientific community has put forward interdisciplinary methodological toolboxes for understanding the components of the boreal forest C balance, including in situ detailed monitoring, remote-sensing observations, and numerical modeling. Some of these

multivariate sources of information were summarized here to illustrate the magnitude and variability of the C balance components in the circumboreal region. The estimates provide only a "static" perspective based on the long-term average boreal forest C balance from the last decades. Attributing how individual aspects of climate change have affected the temporal dynamics of the C balance in the circumboreal region remains uncertain across different levels of spatial organization, spanning from the tissue and tree levels to integrated responses at the forest-stand, landscape, and regional levels.

Climate change manifests itself in the circumboreal region primarily through warmer air temperatures (ACIA, 2005; IPCC 2013; Serreze & Francis, 2006). Such changes directly affect boreal forest structure and function (Gauthier et al., 2015; Soja et al., 2007). Multivariate observations point toward a significant increase in heterotrophic respiration because of increased air temperatures during the last decades (Bond-Lamberty et al., 2018). In addition, warmer temperatures have been associated with a lengthening of the growing season, including shifts in spring and autumn phenology, which results in the *greening* of the circumboreal region and an increase in GEP, and, potentially, NPP (Forkel et al., 2016; Kauppi et al., 2014; Piao et al., 2020; Tagesson et al., 2020; Zhu et al., 2016). However, such patterns have not always been confirmed at local scales, when, for example, tree-ring records are analyzed (Duchesne et al., 2019; Giguère-Croteau et al., 2019; Girardin et al., 2016; Marchand et al., 2018). Furthermore, warmer temperatures in the circumpolar region lead to a northward advance of the boreal forest–tundra transition zone and shrub expansion in tundra ecosystems (Elmendorf et al., 2012; Gareth Rees et al., 2020; Myers-Smith et al., 2011). The beneficial effect of air temperature increases on boreal tree function might be transitory, however, because of additional factors limiting growth and productivity in the long term (Babst et al., 2019; D'Orangeville et al., 2018).

Increasing atmospheric CO_2 concentrations and nitrogen deposition have been associated with a possible stimulation of tree growth, i.e., the fertilization effect and the greening of the Northern Hemisphere. This CO_2 fertilization effect implies that other factors affecting forest productivity were partially or not at all limiting. This viewpoint has been challenged recently (Peñuelas et al., 2017; Wang et al., 2020) because additional factors are likely limiting tree growth beyond C availability, including nutrient and water limitations (Peters et al., 2021; Yuan et al., 2019). The projected changes in major climatic variables are expected to shift tree growth climate sensitivity in boreal forests, e.g., reducing the importance of temperature/energy limitations and increasing the importance of water limitations (Babst et al., 2019; D'Orangeville et al., 2018), potentially altering C turnover rates and sink strength. The land C sink results from the interplay between C assimilation and respiration; thus, the net result of changes in climatic variables in the boreal forest C balance and sink strength remains uncertain (Naidu & Bagchi, 2021; Schurgers et al., 2018; Zhu et al., 2019).

Forest productivity (and tree growth) is a key aspect that contributes to the forest C balance and the C sink strength, but it is not the only one. An increase in productivity does not necessarily translate into an increase in forest C sink strength. The

latter depends largely on the C residence times, i.e., at the tree level, to which tissues/compartments the assimilated C will be allocated (e.g., long-lived tissues like stemwood or short-lived tissues such as leaves and fine roots) or at the forest-stand or larger spatial scales, to the frequency and intensity of natural disturbances (e.g., fires, insects, tree mortality) and forest management strategies. The interplay of residence times, e.g., turnover rates, and productivity, e.g., tree growth, ultimately controls the long-term C source-sink strength (Harmon, 2001; Körner, 2017; Peñuelas et al., 2017). The two processes often present a positive covariation at the tree level, i.e., fast-growing strategies are also associated with faster turnover rates (lower longevity; Brienen et al., 2020; Reich, 2014). Yet, at the ecosystem level, stand demography and community interactions shape the net effect, making extrapolations of the forest C sink strength challenging when done solely on the basis of tree physiology (Anderegg et al., 2020; Harmon, 2001; McDowell et al., 2020). Although the boreal forest land-scapes have always been dynamic, reports now cite changes in the frequency and intensity of disturbances such as wildfires, insect outbreaks, and droughts (Bond-Lamberty et al., 2007; Brandt et al., 2013; Goetz et al., 2012; Peng et al., 2011) or chronic changes in forest structure and function because of permafrost thaw (e.g., Helbig et al., 2016). When combined with management practices (harvesting; Ameray et al., 2021; Ceccherini et al., 2020), such changes can substantially affect the C balance of the circumboreal region and C sink strength (Seidl et al., 2020).

Although aboveground tree growth only represents a minor fraction of the forest C balance in the boreal region, because of low productivity and a short growing season, aboveground physiological processes trigger numerous feedbacks of belowground components, e.g., energy partitioning/albedo feedback and thus regulation of soil temperature. Furthermore, tree growth represents a major C-storing compartment for climate-meaningful time scales and contributes to the main inflow of C from the atmosphere to belowground C pools and to ecosystem-level C dynamics. A holistic monitoring and modeling approach is required to better constrain future trajectories of C in boreal ecosystems and delineate climate-sustainable forest management strategies. This can be better achieved with partitioned estimates of the C balance components as summarized in this study.

References

ACIA. (2005). *Impacts of a warming arctic: Arctic climate impact assessment*. Cambridge University Press.

Alexander, H. D., Mack, M. C., Goetz, S., et al. (2012). Carbon accumulation patterns during post-fire succession in cajander larch (*Larix cajanderi*) forests of siberia. *Ecosystems, 15*(7), 1065–1082. https://doi.org/10.1007/s10021-012-9567-6.

Ameray, A., Bergeron, Y., Valeria, O., et al. (2021). Forest carbon management: A review of silvicultural practices and management strategies across boreal, temperate and tropical forests. *Current Forestry Reports* , *7*(4), 245–266. https://doi.org/10.1007/s40725-021-00151-w.

Amiro, B.D., Barr, A. G., Barr, J. G. et al. (2010). Ecosystem carbon dioxide fluxes after disturbance in forests of North America. *Journal of Geophysical Research: Biogeosciences*, *115*(G4), G00K02 https://doi.org/10.1029/2010JG001390.

Anderegg, W. R. L., Trugman, A. T., Badgley, G., et al. (2020). Climate-driven risks to the climate mitigation potential of forests. *Science*, *368*(6497), eaaz7005 https://doi.org/10.1126/science.aaz 7005.

Anderson-Teixeira, K. J., Davies, S. J., Bennett, A. C., et al. (2015). CTFS-ForestGEO: A worldwide network monitoring forests in an era of global change. *Global Change Biology, 21*(2), 528–549. https://doi.org/10.1111/gcb.12712.

Babst, F., Bouriaud, O., Alexander, R., et al. (2014a). Toward consistent measurements of carbon accumulation: A multi-site assessment of biomass and basal area increment across Europe. *Dendrochronologia, 32*(2), 153–161. https://doi.org/10.1016/j.dendro.2014.01.002.

Babst, F., Bouriaud, O., Papale, D., et al. (2014b). Above-ground woody carbon sequestration measured from tree rings is coherent with net ecosystem productivity at five eddy-covariance sites. *New Phytologist, 201*(4), 1289–1303. https://doi.org/10.1111/nph.12589.

Babst, F., Friend, A. D., Karamihalaki, M., et al. (2021). Modeling ambitions outpace observations of forest carbon allocation. *Trends in Plant Science, 26*(3), 210–219. https://doi.org/10.1016/j.tpl ants.2020.10.002.

Babst, F., Bouriaud, O., Poulter, B. et al. (2019). Twentieth century redistribution in climatic drivers of global tree growth. *Science Advances*, *5*(1), eaat4313. https://doi.org/10.1126/sciadv.aat4313.

Baldocchi, D. D. (2020). How eddy covariance flux measurements have contributed to our understanding of *Global Change Biology*. *Global Change Biology, 26*(1), 242–260. https://doi.org/10.1111/gcb.14807.

Baldocchi, D., & Peñuelas, J. (2019). The physics and ecology of mining carbon dioxide from the atmosphere by ecosystems. *Global Change Biology, 25*(4), 1191–1197. https://doi.org/10.1111/gcb.14559.

Bar-On, Y. M., Phillips, R., & Milo, R. (2018). The biomass distribution on Earth. *Proceedings of the National Academy of Sciences of the United States of America*, *115*(25), 6506–6511. https://doi.org/10.1073/pnas.1711842115.

Barr, A. G., van der Kamp, G., Black, T. A., et al. (2012). Energy balance closure at the BERMS flux towers in relation to the water balance of the white gull creek watershed 1999–2009. *Agricultural and Forest Meteorology, 153*, 3–13. https://doi.org/10.1016/j.agrformet.2011.05.017.

Bonan, G. B. (2008). Forests and climate change: Forcings, feedbacks, and the climate benefits of forests. *Science, 320*(5882), 1444–1449. https://doi.org/10.1126/science.1155121.

Bonan, G. B. (2016). Forests, climate, and public policy: A 500-year interdisciplinary odyssey. *Annual Review of Ecology, Evolution, and Systematics, 47*, 97–121. https://doi.org/10.1146/ann urev-ecolsys-121415-032359.

Bond-Lamberty, B., Peckham, S. D., Ahl, D. E., et al. (2007). Fire as the dominant driver of central Canadian boreal forest carbon balance. *Nature, 450*(7166), 89–92. https://doi.org/10.1038/nature 06272.

Bond-Lamberty, B., Bailey, V. L., Chen, M., et al. (2018). Globally rising soil heterotrophic respiration over recent decades. *Nature, 560*(7716), 80–83. https://doi.org/10.1038/s41586-018-0358-x.

Bradshaw, C. J. A., & Warkentin, I. G. (2015). Global estimates of boreal forest carbon stocks and flux. *Global and Planetary Change*, *128*, 24–30. https://doi.org/10.1016/j.gloplacha.2015.02.004.

Brandt, J. P., Flannigan, M. D., Maynard, D. G., et al. (2013). An introduction to Canada's boreal zone: Ecosystem processes, health, sustainability, and environmental issues. *Environmental Reviews, 21*(4), 207–226. https://doi.org/10.1139/er-2013-0040.

Brassard, B. W., & Chen, H. Y. H. (2006). Stand structural dynamics of North American boreal forests. *Critical Reviews in Plant Sciences, 25*(2), 115–137. https://doi.org/10.1080/073526805 00348857.

Brienen, R. J. W., Caldwell, L., Duchesne, L., et al. (2020). Forest carbon sink neutralized by pervasive growth-lifespan trade-offs. *Nature Communications, 11*(1), 4241. https://doi.org/10.1038/s41467-020-17966-z.

Bugmann, H., & Bigler, C. (2011). Will the CO_2 fertilization effect in forests be offset by reduced tree longevity? *Oecologia, 165*(2), 533–544. https://doi.org/10.1007/s00442-010-1837-4.

Büntgen, U., Krusic, P. J., Piermattei, A., et al. (2019). Limited capacity of tree growth to mitigate the global greenhouse effect under predicted warming. *Nature Communications, 10*(1), 2171. https://doi.org/10.1038/s41467-019-10174-4.

Campioli, M., Malhi, Y., Vicca, S., et al. (2016). Evaluating the convergence between eddy-covariance and biometric methods for assessing carbon budgets of forests. *Nature Communications, 7*(5), 13717. https://doi.org/10.1038/ncomms13717.

Carvalhais, N., Forkel, M., Khomik, M., et al. (2014). Global covariation of carbon turnover times with climate in terrestrial ecosystems. *Nature, 514*(7521), 213–217. https://doi.org/10.1038/nature13731.

Ceccherini, G., Duveiller, G., Grassi, G., et al. (2020). Abrupt increase in harvested forest area over Europe after 2015. *Nature, 583*(7814), 72–77. https://doi.org/10.1038/s41586-020-2438-y.

Chapin, F. S., III. (1980). The mineral nutrition of wild plants. *Annual Review of Ecology and Systematics, 11*, 233–260. https://doi.org/10.1146/annurev.es.11.110180.001313.

Chapin, F. S., III., Woodwell, G. M., Randerson, J. T., et al. (2006). Reconciling carbon-cycle concepts, terminology, and methods. *Ecosystems, 9*(7), 1041–1050. https://doi.org/10.1007/s10021-005-0105-7.

Chen, J. M., Govind, A., Sonnentag, O., et al. (2006). Leaf area index measurements at Fluxnet-Canada forest sites. *Agricultural and Forest Meteorology, 140*(1–4), 257–268. https://doi.org/10.1016/j.agrformet.2006.08.005.

Ciais, P., Tan, J., Wang, X., et al. (2019). Five decades of northern land carbon uptake revealed by the interhemispheric CO_2 gradient. *Nature, 568*(7751), 221–225. https://doi.org/10.1038/s41586-019-1078-6.

Clark, D. A., Brown, S., Kicklighter, D. W., et al. (2001). Measuring net primary production in forests: Concepts and field methods. *Ecological Applications, 11*(2), 356–370. https://doi.org/10.1890/1051-0761(2001)011[0356:MNPPIF]2.0.CO;2.

Clemmensen, K. E., Bahr, A., Ovaskainen, O., et al. (2013). Roots and associated fungi drive long-term carbon sequestration in boreal forest. *Science* 339(6127), 1615–1618 https://doi.org/10.1016/b978-0-408-01434-2.50020-6; https://doi.org/10.1126/science.1231923.

Collalti, A., & Prentice, I. C. (2019). Is NPP proportional to GPP? Waring's hypothesis 20 years on. *Tree Physiology, 39*(8), 1473–1483. https://doi.org/10.1093/treephys/tpz034.

Cook-Patton, S. C., Leavitt, S. M., Gibbs, D., et al. (2020). Mapping carbon accumulation potential from global natural forest regrowth. *Nature, 585*(7826), 545–550. https://doi.org/10.1038/s41586-020-2686-x.

Crowther, T. W., Glick, H. B., Covey, K. R., et al. (2015). Mapping tree density at a global scale. *Nature, 525*(7568), 201–205. https://doi.org/10.1038/nature14967.

De Lucia, E. H., Drake, J. E., Thomas, R. B., et al. (2007). Forest carbon use efficiency: Is respiration a constant fraction of gross primary production? *Global Change Biology, 13*(6), 1157–1167. https://doi.org/10.1111/j.1365-2486.2007.01365.x.

Dewar, R. C., Medlyn, B. E., & McMurtrie, R. E. (1998). A mechanistic analysis of light and carbon use efficiencies. *Plant, Cell and Environment, 21*(6), 573–588. https://doi.org/10.1046/j.1365-3040.1998.00311.x.

D'Orangeville, L., Houle, D., Duchesne, L., et al. (2018). Beneficial effects of climate warming on boreal tree growth may be transitory. *Nature Communications, 9*(1), 3213. https://doi.org/10.1038/s41467-018-05705-4.

Drake, J. E., Tjoelker, M. G., Aspinwall, M. J., et al. (2019). The partitioning of gross primary production for young *Eucalyptus tereticornis* trees under experimental warming and altered water availability. *New Phytologist*, *222*(3), 1298–1312. https://doi.org/10.1111/nph.15629.

Duchesne, L., Houle, D., Ouimet, R., et al. (2019). Large apparent growth increases in boreal forests inferred from tree-rings are an artefact of sampling biases. *Scientific Reports*, *9*(1), 6832. https://doi.org/10.1038/s41598-019-43243-1.

Duncanson, L., Armston, J., Disney, M., et al. (2019). The importance of consistent global forest aboveground biomass product validation. *Surveys in Geophysics, 40*(4), 979–999. https://doi.org/10.1007/s10712-019-09538-8.

Elmendorf, S. C., Henry, G. H. R., Hollister, R. D., et al. (2012). Plot-scale evidence of tundra vegetation change and links to recent summer warming. *Nature Climate Change*, *2*(6), 453–457. https://doi.org/10.1038/nclimate1465.

Farquhar, G. D., von Caemmerer, S., & Berry, J. A. (1980). A biochemical model of photosynthetic CO_2 assimilation in leaves of C3 species. *Planta, 149*(1), 78–90. https://doi.org/10.1007/BF00386231.

Fatichi, S., Pappas, C., Zscheischler, J., et al. (2019). Modelling carbon sources and sinks in terrestrial vegetation. *New Phytologist*, *221*(2), 652–668. https://doi.org/10.1111/nph.15451.

Fick, S. E., & Hijmans, R. J. (2017). WorldClim 2: New 1-km spatial resolution climate surfaces for global land areas. *International Journal of Climatology, 37*, 4302–4315. https://doi.org/10.1002/joc.5086.

Forkel, M., Carvalhais, N., Rödenbeck, C., et al. (2016). Enhanced seasonal CO_2 exchange caused by amplified plant productivity in northern ecosystems. *Science, 351*(6274), 696–699. https://doi.org/10.1126/science.aac4971.

Friedlingstein, P., O'Sullivan, M., Jones, M. W., et al. (2020). Global carbon budget 2020. *Earth System Science Data, 12*(4), 3269–3340. https://doi.org/10.5194/essd-12-3269-2020.

Friedlingstein, P. (2015). Carbon cycle feedbacks and future climate change. *Philosophical Transactions of the Royal Society A: Mathematical, Physical and Engineering Sciences*, *373*, 1–22 https://doi.org/10.1098/not.

Friend, A. D., Lucht, W., Rademacher, T. T., et al. (2014). Carbon residence time dominates uncertainty in terrestrial vegetation responses to future climate and atmospheric CO_2. *Proceedings of the National Academy of Sciences of the United States of America*, *111*(9), 3280. https://doi.org/10.1073/pnas.1222477110.

Gaumont-Guay, D., Black, T. A., Barr, A. G., et al. (2014). Eight years of forest-floor CO_2 exchange in a boreal black spruce forest: Spatial integration and long-term temporal trends. *Agricultural and Forest Meteorology, 184*, 25–35. https://doi.org/10.1016/j.agrformet.2013.08.010.

Gauthier, S., Bernier, P., Kuuluvainen, T., et al. (2015). Boreal forest health and global change. *Science, 349*, 819–822. https://doi.org/10.1126/science.aaa9092.

Giguère-Croteau, C., Boucher, É., Bergeron, Y., et al. (2019). North America's oldest boreal trees are more efficient water users due to increased [CO_2], but do not grow faster. *Proceedings of the National Academy of Sciences of the United States of America*, *116*(7), 2749–2754. https://doi.org/10.1073/pnas.1816686116.

Girardin, M. P., Bouriaud, O., Hogg, E. H., et al. (2016). No growth stimulation of Canada's boreal forest under half-century of combined warming and CO_2 fertilization. *Proceedings of the National Academy of Sciences of the United States of America*, *113*(52), E8406–E8414. https://doi.org/10.1073/pnas.1610156113.

Goetz, S. J., Bond-Lamberty, B., Law, B. E., et al. (2012). Observations and assessment of forest carbon dynamics following disturbance in North America. *Journal of Geophysical Research, 117*(G2), G02022. https://doi.org/10.1029/2011JG001733.

Gower, S. T., Vogel, J. G., Norman, M. et al. (1997). Carbon distribution and aboveground net primary production in aspen, jack pine, and black spruce stands in Saskatchewan and Manitoba, Canada. *Journal of Geophysical Research*, *102*(D24), 29029–29041. https://doi.org/10.1029/97JD02317.

Grassi, G., House, J., Kurz, W. A., et al. (2018). Reconciling global-model estimates and country reporting of anthropogenic forest CO_2 sinks. *Nature Climate Change*, *8*(10), 914–920. https://doi.org/10.1038/s41558-018-0283-x.

Griffis, T. J., Black, T. A., Morgenstern, K., et al. (2003). Ecophysiological controls on the carbon balances of three southern boreal forests. *Agricultural and Forest Meteorology, 117*(1–2), 53–71. https://doi.org/10.1016/S0168-1923(03)00023-6.

Harmon, M. E. (2001). Carbon sequestration in forest; addressing the scale question. *Journal of Forestry, 99*, 24–29. https://doi.org/10.1093/jof/99.4.24.

Hart, S. A., & Chen, H. Y. H. (2006). Understory vegetation dynamics of North American boreal forests. *Critical Reviews in Plant Sciences, 25*(4), 381–397. https://doi.org/10.1080/073526806 00819286.

Helbig, M., Pappas, C., & Sonnentag, O. (2016). Permafrost thaw and wildfire: Equally important drivers of boreal tree cover changes in the Taiga Plains, Canada. *Geophysical Research Letters, 43*(4), 1598–1606. https://doi.org/10.1002/2015GL067193.

Ilvesniemi, H., Levula, J., Ojansuu, R., et al. (2009). Long-term measurements of the carbon balance of a boreal Scots pine dominated forest ecosystem. *Boreal Environment Research, 14*(4), 731–753.

Intergovernmental Panel on Climate Change (IPCC). (2013). *Climate change 2013: The physical science basis. Contribution of Working Group I to the fifth assessment report of the Intergovernmental Panel on Climate Change.* Cambridge: Cambridge University Press.

Kajimoto, T., Osawa, A., Usoltsev, V. A., et al. (2010). Biomass and productivity of Siberian larch forest ecosystems. In A. Osawa, O. A. Zyryanova, Y. Matsuura, T. Kajimoto, R. W. Wein (Eds.), *Permafrost ecosystems: Siberian larch forests.* Ecological Studies 209 (pp. 99–122). Dordrecht: Springer.

Kauppi, P. E., Posch, M., & Pirinen, P. (2014). Large impacts of climatic warming on growth of boreal forests since 1960. *PLoS ONE, 9*(11), e111340. https://doi.org/10.1371/journal.pone.011 1340.

Keenan, T. F., & Williams, C. A. (2018). The terrestrial carbon sink. *Annual Review of Environment and Resources, 43*(1), 219–243. https://doi.org/10.1146/annurev-environ-102017-030204.

Kolari, P., Kulmala, L., Pumpanen, J., et al. (2009). CO_2 exchange and component CO_2 fluxes of a boreal Scots pine forest. *Boreal Environment Research, 14*(4), 761–783.

Körner, C. (2017). A matter of tree longevity. *Science, 355*(6321), 130–131. https://doi.org/10.1126/science.aal2449.

Körner, C. (2018). Concepts in empirical plant ecology. *Plant Ecology Diversity, 11*(4), 405–428. https://doi.org/10.1080/17550874.2018.1540021.

Kotani, A., Kononov, A. V., Ohta, T., et al. (2014). Temporal variations in the linkage between the net ecosystem exchange of water vapour and CO_2 over boreal forests in eastern Siberia. *Ecohydrology, 7*(2), 209–225. https://doi.org/10.1002/eco.1449.

Krishnan, P., Black, T. A., Barr, A. G., et al. (2008). Factors controlling the interannual variability in the carbon balance of a southern boreal black spruce forest. *Journal of Geophysical Research, 113*(D9), D09109. https://doi.org/10.1029/2007JD008965.

Kurz, W. A., Shaw, C. H., Boisvenue, C., et al. (2013). Carbon in Canada's boreal forest–A synthesis. *Environmental Reviews, 21*(4), 260–292. https://doi.org/10.1139/er-2013-0041.

Lagergren, F., Jönsson, A. M., Linderson, H., et al. (2019). Time shift between net and gross CO_2 uptake and growth derived from tree rings in pine and spruce. *Trees, 33*(3), 765–776. https://doi.org/10.1007/s00468-019-01814-9.

Landsberg, J. J., Waring, R. H., & Williams, M. (2020). The assessment of NPP/GPP ratio. *Tree Physiology, 40*(6), 695–699. https://doi.org/10.1093/treephys/tpaa016.

Le Quéré, C., Andrew, R. M., Friedlingstein, P., et al. (2018). Global carbon budget 2017. *Earth System Science Data, 10*(1), 405–448. https://doi.org/10.5194/essd-10-405-2018.

Litton, C. M., Raich, J. W., & Ryan, M. G. (2007). Carbon allocation in forest ecosystems. *Global Change Biology, 13*(10), 2089–2109. https://doi.org/10.1111/j.1365-2486.2007.01420.x.

Liu, P., Black, T. A., Jassal, R. S., et al. (2019). Divergent long-term trends and interannual variation in ecosystem resource use efficiencies of a southern boreal old black spruce forest 1999–2017. *Global Change Biology, 25*(9), 3056–3069. https://doi.org/10.1111/gcb.14674.

Lloyd, J., Shibistova, O., Zolotoukhine, D., et al. (2002). Seasonal and annual variations in the photosynthetic productivity and carbon balance of a central Siberian pine forest. *Tellus B Chemical and Physical Meteorology*, *54*(5), 590–610. https://doi.org/10.3402/tellusb.v54i5.16689.

Malhi, Y., Baldocchi, D. D., & Jarvis, P. G. (1999). The carbon balance of tropical, temperate and boreal forests. *Plant, Cell and Environment, 22*(6), 715–740. https://doi.org/10.1046/j.1365-3040.1999.00453.x.

Manzoni, S., Čapek, P., Porada, P., et al. (2018). Reviews and syntheses: Carbon use efficiency from organisms to ecosystems–definitions, theories, and empirical evidence. *Biogeosciences, 15*(19), 5929–5949. https://doi.org/10.5194/bg-15-5929-2018.

Marchand, W., Girardin, M. P., Gauthier, S., et al. (2018). Untangling methodological and scale considerations in growth and productivity trend estimates of Canada's forests. *Environmental Research Letters, 13*(9), 093001. https://doi.org/10.1088/1748-9326/aad82a.

McDowell, N. G., Allen, C. D., Anderson-Teixeira, K., et al. (2020). Pervasive shifts in forest dynamics in a changing world. *Science*, *368*(6494), eaaz9463. https://doi.org/10.1126/science.aaz9463.

Mencuccini, M., & Bonosi, L. (2001). Leaf/sapwood area ratios in Scots pine show acclimation across Europe. *Canadian Journal of Forest Research, 31*(3), 442–456. https://doi.org/10.1139/x00-173.

Myers-Smith, I. H., Forbes, B. C., Wilmking, M., et al. (2011). Shrub expansion in tundra ecosystems: Dynamics, impacts and research priorities. *Environmental Research Letters, 6*(4), 045509. https://doi.org/10.1088/1748-9326/6/4/045509.

Naidu, D. G. T., & Bagchi, S. (2021). Greening of the earth does not compensate for rising soil heterotrophic respiration under climate change. *Global Change Biology, 27*(10), 2029–2038. https://doi.org/10.1111/gcb.15531.

Odum, E. P. (1969). The strategy of ecosystem development. *Science, 164*(3877), 262–270. https://doi.org/10.1126/science.164.3877.262.

Ohta, T., Maximov, T. C., Dolman, A. J., et al. (2008). Interannual variation of water balance and summer evapotranspiration in an eastern Siberian larch forest over a 7-year period (1998–2006). *Agricultural and Forest Meteorology, 148*(12), 1941–1953. https://doi.org/10.1016/j.agrformet.2008.04.012.

Ohta, T., Kotani, A., Iijima, Y., et al. (2014). Effects of waterlogging on water and carbon dioxide fluxes and environmental variables in a Siberian larch forest, 1998–2011. *Agricultural and Forest Meteorology, 188*, 64–75. https://doi.org/10.1016/j.agrformet.2013.12.012.

Pan, Y., Birdsey, R., Phillips, O. L., et al. (2013). The structure, distribution, and biomass of the world's forests. *Annual Review of Ecology, Evolution, and Systematics, 44*(1), 593–622. https://doi.org/10.1146/annurev-ecolsys-110512-135914.

Pappas, C., Maillet, J., Rakowski, S., et al. (2020). Aboveground tree growth is a minor and decoupled fraction of boreal forest carbon input. *Agricultural and Forest Meteorology, 290*, 108030. https://doi.org/10.1016/j.agrformet.2020.108030.

Pastorello, G., Trotta, C., Canfora, E., et al. (2020). The FLUXNET2015 dataset and the ONEFlux processing pipeline for eddy covariance data. *Scientific Data, 7*(1), 225. https://doi.org/10.1038/s41597-020-0534-3.

Peng, C., Ma, Z., Lei, X., et al. (2011). A drought-induced pervasive increase in tree mortality across Canada's boreal forests. *Nature Climate Change*, *1*, 467–471. https://doi.org/10.1038/nclimate1293.

Peñuelas, J., Ciais, P., Canadell, J. G., et al. (2017). Shifting from a fertilization-dominated to a warming-dominated period. *Nature Ecology and Evolution, 1*(10), 1438–1445. https://doi.org/10.1038/s41559-017-0274-8.

Peters, R. L., Steppe, K., Cuny, H. E., et al. (2021). Turgor-a limiting factor for radial growth in mature conifers along an elevational gradient. *New Phytologist, 229*(1), 213–229. https://doi.org/10.1111/nph.16872.

Piao, S., Wang, X., Park, T., et al. (2020). Characteristics, drivers and feedbacks of global greening. *Nature Reviews Earth and Environment, 1*(1), 14–27. https://doi.org/10.1038/s43017-019-0001-x.

Popkin, G. (2019). How much can forests fight climate change? *Nature, 565*, 280–282. https://doi.org/10.1038/d41586-019-00122-z.

Pugh, T. A. M., Arneth, A., Kautz, M., et al. (2019a). Important role of forest disturbances in the global biomass turnover and carbon sinks. *Nature Geoscience, 12*(9), 730–735. https://doi.org/10.1038/s41561-019-0427-2.

Pugh, T. A. M., Lindeskog, M., Smith, B., et al. (2019b). Role of forest regrowth in global carbon sink dynamics. *Proceedings of the National Academy of Sciences of the United States of America, 116*(10), 4382–4387. https://doi.org/10.1073/pnas.1810512116.

Pumpanen, J., Kulmala, L., Lindén, A., et al. (2015). Seasonal dynamics of autotrophic respiration in boreal forest soil estimated by continuous chamber measurements. *Boreal Environment Research, 20*(5), 637–650.

Rannik, Ü., Altimir, N., Raittila, J., et al. (2002). Fluxes of carbon dioxide and water vapour over Scots pine forest and clearing. *Agricultural and Forest Meteorology, 111*(3), 187–202. https://doi.org/10.1016/S0168-1923(02)00022-9.

Rees, W. G., Hofgaard, A., Boudreau, S., et al. (2020). Is subarctic forest advance able to keep pace with climate change? *Global Change Biology, 26*(7), 3965–3977. https://doi.org/10.1111/gcb.15113.

Reich, P. (2014). The world-wide "fast-slow" plant economics spectrum: A traits manifesto. *Journal of Ecology, 102*, 275–301. https://doi.org/10.1111/1365-2745.12211.

Reichstein, M., Falge, E., Baldocchi, D., et al. (2005). On the separation of net ecosystem exchange into assimilation and ecosystem respiration: Review and improved algorithm. *Global Change Biology, 11*(9), 1424–1439. https://doi.org/10.1111/j.1365-2486.2005.001002.x.

Reichstein, M., Bahn, M., Ciais, P., et al. (2013). Climate extremes and the carbon cycle. *Nature, 500*(7462), 287–295. https://doi.org/10.1038/nature12350.

Rodríguez-Veiga, P., Quegan, S., Carreiras, J., et al. (2019). Forest biomass retrieval approaches from earth observation in different biomes. *International Journal of Applied Earth Observation and Geoinformation, 77*, 53–68. https://doi.org/10.1016/j.jag.2018.12.008.

Running, S., & Zhao, M. (2019). MOD17A3HGF MODIS/Terra net primary production gap-filled yearly L4 Global 500 m SIN Grid V006. NASA EOSDIS Land Processes DAAC.

Sawamoto, T., Hatano, R., Shibuya, M., et al. (2003). Changes in net ecosystem production associated with forest fire in taiga ecosystems, near Yakutsk, Russia. *Soil Science and Plant Nutrition, 49*(4), 493–501. https://doi.org/10.1080/00380768.2003.10410038.

Schepaschenko, D., Chave, J., Phillips, O. L., et al. (2019). The forest observation system, building a global reference dataset for remote sensing of forest biomass. *Scientific Data, 6*(1), 198. https://doi.org/10.1038/s41597-019-0196-1.

Schurgers, G., Ahlstrom, A., Arneth, A., et al. (2018). Climate sensitivity controls uncertainty in future terrestrial carbon sink. *Geophysical Research Letters, 45*(9), 4329–4336. https://doi.org/10.1029/2018GL077528.

Seidl, R., Thom, D., Kautz, M., et al. (2017). Forest disturbances under climate change. *Nature Climate Change, 7*(6), 395–402. https://doi.org/10.1038/nclimate3303.

Seidl, R., Honkaniemi, J., Aakala, T., et al. (2020). Globally consistent climate sensitivity of natural disturbances across boreal and temperate forest ecosystems. *Ecography, 43*(7), 967–978. https://doi.org/10.1111/ecog.04995.

Serreze, M. C., & Francis, J. A. (2006). The Arctic amplification debate. *Climatic Change, 76*(3–4), 241–264. https://doi.org/10.1007/s10584-005-9017-y.

Soja, A. J., Tchebakova, N. M., French, N. H. F., et al. (2007). Climate-induced boreal forest change: Predictions versus current observations. *Global and Planetary Change, 56*, 274–296. https://doi.org/10.1016/j.gloplacha.2006.07.028.

Tagesson, T., Schurgers, G., Horion, S., et al. (2020). Recent divergence in the contributions of tropical and boreal forests to the terrestrial carbon sink. *Nature Ecology and Evolution, 4*(2), 202–209. https://doi.org/10.1038/s41559-019-1090-0.

Tei, S., Sugimoto, A., Kotani, A., et al. (2019). Strong and stable relationships between tree-ring parameters and forest-level carbon fluxes in a Siberian larch forest. *Polar Science, 21*(1), 146–157. https://doi.org/10.1016/j.polar.2019.02.001.

Thurner, M., Beer, C., Santoro, M., et al. (2014). Carbon stock and density of northern boreal and temperate forests. *Global Ecology and Biogeography, 23*(3), 297–310. https://doi.org/10.1111/geb.12125.

Trumbore, S., Brando, P., & Hartmann, H. (2015). Forest health and global change. *Science, 349*(6250), 814–818. https://doi.org/10.1126/science.aac6759.

Van Oijen, M., Schapendonk, A., & Höglind, M. (2010). On the relative magnitudes of photosynthesis, respiration, growth and carbon storage in vegetation. *Annals of Botany, 105*(5), 793–797. https://doi.org/10.1093/aob/mcq039.

Vesala, T., Suni, T., Rannik, Ü., et al. (2005). Effect of thinning on surface fluxes in a boreal forest. *Global Biogeochemical Cycles*, 19(2), GB2001. https://doi.org/10.1029/2004GB002316.

Vicca, S., Luyssaert, S., Peñuelas, J., et al. (2012). Fertile forests produce biomass more efficiently. *Ecology Letters, 15*(6), 520–526. https://doi.org/10.1111/j.1461-0248.2012.01775.x.

Wang, S., Zhang, Y., Ju, W., et al. (2020). Recent global decline of CO_2 fertilization effects on vegetation photosynthesis. *Science, 370*(6522), 1295–1300. https://doi.org/10.1126/science.abb7772.

Waring, R. H., Landsberg, J. J., & Williams, M. (1998). Net primary production of forests: A constant fraction of gross primary production? *Tree Physiology, 18*(2), 129–134. https://doi.org/10.1093/treephys/18.2.129.

Yu, K., Smith, W. K., Trugman, A. T., et al. (2019). Pervasive decreases in living vegetation carbon turnover time across forest climate zones. *Proceedings of the National Academy of Sciences of the United States of America*, 116(49), 24662–24667. https://doi.org/10.1073/pnas.1821387116.

Yuan, W., Zheng, Y., Piao, S., et al. (2019). Increased atmospheric vapor pressure deficit reduces global vegetation growth. *Science Advances*, 5(8), eaax1396. https://doi.org/10.1126/sciadv.aax1396.

Zeng, J., Matsunaga, T., Tan, Z. H., et al. (2020). Global terrestrial carbon fluxes of 1999–2019 estimated by upscaling eddy covariance data with a random forest. *Scientific Data, 7*(1), 313. https://doi.org/10.1038/s41597-020-00653-5.

Zhu, Z., Piao, S., Myneni, R. B., et al. (2016). Greening of the earth and its drivers. *Nature Climate Change*, 6(8), 791–795. https://doi.org/10.1038/nclimate3004.

Zhu, P., Zhuang, Q., Welp, L., et al. (2019). Recent warming has resulted in smaller gains in net carbon uptake in northern high latitudes. *Journal of Climate, 32*(18), 5849–5863. https://doi.org/10.1175/jcli-d-18-0653.1.